第 27 卷第 5 期 无 机 化 学 学 报 Vol.27 No.5
2011 年 5 月 CHINESE JOURNAL OF INORGANIC CHEMISTRY 1001-1007

碳纳米管含量对炭炭复合材料组织及力学性能的影响

李克智* 宋 强 武立言 李贺军 弓巧娟
(西北工业大学凝固技术国家重点实验室,西安 710072)

摘要:炭纤维上原位合成了均匀生长且具有伸张形貌的碳纳米管,借助化学气相渗透制备了碳纳米管增强的炭炭复合材料,研究了不同含量的碳纳米管对炭炭复合材料组织和力学性能的影响。结果表明:炭纤维上生长碳纳米管改变了热解炭的沉积行为,诱导了各向同性热解炭的生成,且随着碳纳米管含量的增加,各向同性热解炭的厚度增加,但是复合材料的 d_{002} 值却明显降低。微量的碳纳米管即可显著提高复合材料的力学强度,随着其含量的增加,复合材料的力学强度和模量迅速提高,但材料的断裂行为却急剧恶化,断裂模式由最初的假塑性断裂转变为脆性断裂。

关键词:炭炭复合材料;碳纳米管;杂交;微观组织;力学性能
中图分类号:O613.71;TB331 **文献标识码**:A **文章编号**:1001-4861(2011)05-1001-07

Influence of Carbon Nanotube Content on Microstructures and Mechanical Properties of Carbon/Carbon Composite

LI Ke-Zhi* SONG Qiang WU Li-Yan LI He-Jun GONG Qiao-Juan
(*State Key Laboratory of Solidification Processing, Northwestern Polytechnical University, Xi'an* 710072, *China*)

Abstract: Carbon nanotubes (CNTs) with a uniform growing and extending morphology were *in situ* grown on carbon fibers in carbon felt and then chemical vapor infiltration (CVI) was used to densify the felt to get a CNT-reinforced carbon/carbon (C/C) composite. The influences of CNTs on microstructures and mechanical properties of C/C composite were investigated by varying CNT content. The results show that a layer of isotropic (ISO) pyrocarbon is deposited closely around carbon fibers after growing CNTs and this zone becomes extended with CNTs increase, while the d_{002} value of pyrocarbon decreases for CNT-related composites remarkably. Compared with pure C/C composite, CNT-reinforced C/C composites have much higher mechanical strength and modulus. However, with CNTs increase, the ductility of the composite deteriorates gradually according to the decrease of ductility factor (F_D) value and the fracture mode changes from pseudo-plastic fracture to brittle fracture in spite of the sharp increase in both mechanical strength and modulus.

Key words: carbon/carbon composite; carbon nanotube; hybrid; microstructures; mechanical properties

0 Introduction

Carbon/carbon (C/C) composites are new-type high-temperature materials and are widely used in aerospace and automobile industry for their excellent properties, such as light quality, high specific strength, low thermal expansion, high temperature resistance and outstanding corrosion resistance[1-2]. However, the perfo-rmances of C/C composites depend sensitively on matrix types and the nature of interface bonding

收稿日期:2010-11-29。收修改稿日期:2011-02-03。
国家自然科学基金(No.50832004)、国家 973 项目(No.2011CB605806)和西北工业大学凝固技术国家重点实验室科研基金(No.25-TZ-2009)资助项目。
*通讯联系人。E-mail:likezhi@nwpu.edu.cn

between carbon fiber and matrix[3].

Recently, carbon nanotubes (CNTs) have aroused great interests as reinforcement or additive in C/C composites[4-8]. The corresponding studies have shown a great potential of using CNTs to improve the fiber/matrix interface bonding and induce the formation of high-textured pyrocarbons and thus a better property should be expected in CNT-reinforced C/C (CNT-C/C) composite. However, to the best of our knowledge there have been no reports so far related to the real performance and property enhancement of CNT-C/C composite, especially in mechanical properties. This is because that CNTs always tend to stick together during preparation causing an undesirable CNT/matrix interface bonding[9]. Therefore, for maximizing the performance of CNT-C/C composite, CNTs with large length and less entanglement or agglomeration, which can extend into and stiffen the surrounding matrix and provide increased lateral support of the load-bearing fibers[10], should be grafted on carbon fibers. It is in this context that the present study was undertaken. In this work, carbon felt was used as CNT growing substrate considering its wide practical applications. By using a low-cost in situ growing method, CNTs with a uniform growing and extending (or radially-growing) morphology were prepared on carbon fibers in carbon felt. The influences of CNTs on the morphologies and microstructures of pyrocarbon and mechanical properties of C/C composite were studied by varying CNT content.

1 Experimental

Carbon felt with the apparent density of about 0.20 $g \cdot cm^{-3}$, after being oxidized in nitric acid for 10 h at room temperature, was impregnated with $FeSO_4 \cdot 7H_2O$ dissolved in distilled water (the solute concentration was set to 1.0wt% ~2.0wt%) and then dried in air. Subsequently, the felt was loaded into reaction furnace and was heated to 1 000~1 080 ℃ under the protection of Ar. Upon reaching desired temperature, natural gas (NG) was fed at a flow rate of 15~20 $L \cdot h^{-1}$ as carbon source, while the flow rate of Ar was adjusted to 90~110 $L \cdot h^{-1}$. The synthesis time was 2 h and the synthesis pressure was maintained at about 101.325 kPa. In this work, five CNT-hybridized felts were prepared, respectively, containing 0wt%, 1.6wt%, 3.9wt%, 7.2wt% and 15.3wt% CNTs.

Self-made CVI reactor was applied to densify the felts to obtain the C/C composites at 1 080 ℃ under the pressure of 20 kPa, using NG as carbon source and nitrogen as dilute gas. Afterwards, C/C composites were graphitized at 2 300 ℃ for 2 h. Compressive tests were performed on a universal testing machine to determine the mechanical properties, using cuboid specimen (4 mm×4 mm×5 mm). Five specimens were machined from each type of the as-received composites. The tests were carried out with a constant speed of 0.1 $mm \cdot min^{-1}$ at room temperature.

Scanning electron microscope (SEM, JSM-6700F, 5.0 kV, secondary electron image (SEI) was used to measure the morphology of as-grown CNTs and fracture surfaces of composites. High-resolution transmission electron microscope (HRTEM, JEM 3010, 300 kV) was used to investigate the microstructure and crystallinity of as-grown CNTs. Polarized light microscope (PLM, Leica DMLP optical microscope) was used to investigate the morphology of pyrocarbon matrix and Raman spectroscope (RENISHAW in VIA, with 514.5 nm excitation) was used to examine the microcrystal order of pyrocarbon. To analyze the crystal structure (d_{002} and Lc, indicating the interplanar spacing between (002) planes and the stacked thickness of (002) planes), the powder samples of the five different C/C composites after heat treatment were examined by PANalytical Xpert PRO X-ray diffractometer with monochromatic (35 kV, 20 mA) Cu $K\alpha$ radiation (λ=0.154 06 nm) and a θ-2θ scanning mode at 298 K. The starting/ending position (2θ) is 15.017 0°/79.961 0° with a post-source decay (PSD) acquisition mode.

2 Results and discussion

2.1 Morphology and structure of as-grown CNTs

With increase of CNT content in carbon felt, the average length of CNTs changes from 2 μm to over 10 μm, meanwhile, the corresponding coverage of CNTs on carbon fibers becomes relatively dense. Fig.1a shows the SEM morphology of CNTs grown in preformed

$CNT_{7.2}$-C/C composite. As shown, CNTs grown uniformly on carbon fibers have no agglomeration or acutely curly body and most of them extend themselves into the space aloof from carbon fibers. Enlarged image (Fig.1b) shows that the diameter of as-grown CNTs is much uniform and the value is in the range of 90~110 nm, meanwhile, because of the extending morphology (especially for radially-grown CNTs in inset of Fig.1b), a bulky three-dimensional (3D) network structure is formed above the carbon fiber, which can be beneficial to the reinforcement role of CNTs. TEM image (Fig.1a, inset) confirms that the products are hollow nanotubes with clear and smooth walls. The inner diameter and tube-wall thickness are about 25 nm and 35 nm, respectively.

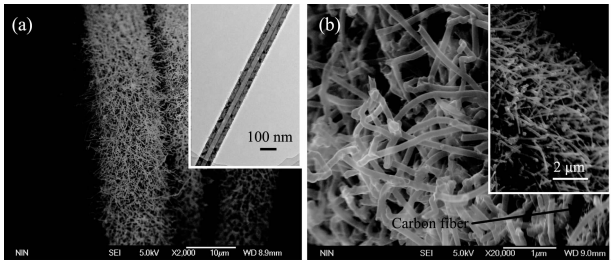

Fig.1　SEM morphology and TEM structure images of as-synthesized CNTs

For maximizing the reinforcing role of CNTs, it is very important and necessary to make CNTs grown with longer length and less entanglement. Although some researches have reported the possibility of synthesizing relatively straight CNTs using alloy catalysts[11-13], the corresponding preparation always involves complex procedures and high cost. In this work, only using iron as catalyst, the radial growth of CNTs with approximately straight body has been found (especially when the CNT content is small). It might be attributed to the relatively big size of iron particles deposited on carbon fibers which have relatively small anisotropy and low surface energy, resulting in the synchronous growth of CNTs in all directions[13].

2.2　Influence of CNTs on morphology and microstructure of C/C composite

Fig.2 shows the PLM images of five composites. For their extinction angle (A_e) values (14°, 13°, 14°, 14° and 11°), the matrix pyrocarbons in all composites are medium/low-textured according to Reznik and Hüttinger [14]. In C/C composite (Fig.2a), however, the pyrocarbons have much larger sizes, fewer growing characteristics (growing cores and boundaries) and much more homocentric annular cracks around carbon fibers than CNT-C/C composites (as shown in Fig.2b~2e). And with increase of CNT content, this morphology distinction in matrix pyrocarbon becomes much bigger and clearer. More interestingly, after growing CNTs on carbon fibers, the fiber/matrix interface has a distinct change in morphology and optical anisotropy (i.e. A_e value). For all CNT-C/C composites, the fiber/matrix interfaces demonstrate a compound and transitional state and their optical anisotropy is much lower than the outer layer pyrocarbons (the pyrocarbons here might be classified as isotropic (ISO) laminar ones according to their very low optical anisotropy). While, in C/C composite, the fiber/matrix interfaces are very tenuous and clear, and the pyrocarbons around them have a similar optical anisotropy to the outer layers. Moreover, with CNTs increasing, the transitional area of ISO pyrocarbon becomes thicker and thicker, especially for $CNT_{15.3}$-C/C composite, the pores among carbon fibers have already been fully infiltrated by this ISO pyrocarbon.

Fig.3a and 3b show the section morphologies of

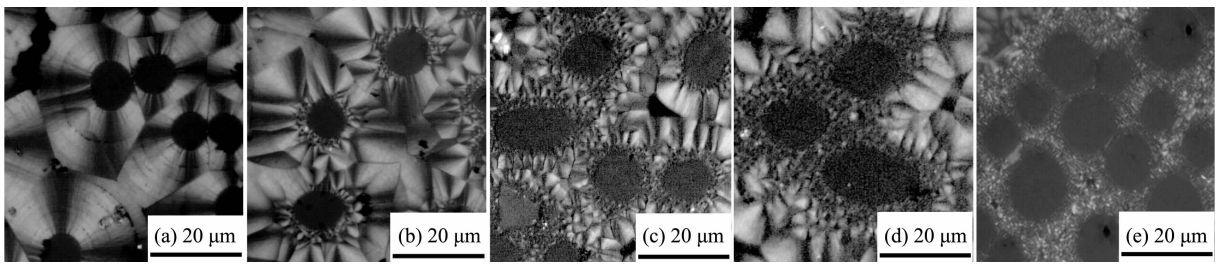

Fig.2　Influence of CNTs on PLM morphology of C/C composite: with increase of CNT content, the growing cores of pyrocarbon become more numerous and the ISO pyrocarbon layer around carbon fibers becomes much thicker

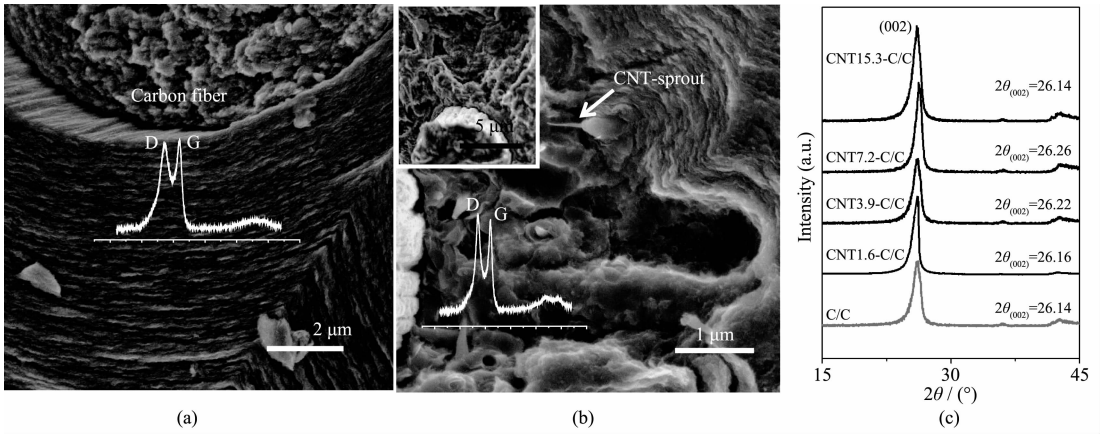

Fig.3 Images and properties of pyrocarbon in different composites: (a) and (b) show the texture of pyrocarbon at fiber/matrix interface and the corresponding Raman spectrum in pure C/C and $CNT_{3.6}$-C/C composites, respectively; inset of (b) is the texture of pyrocarbon in $CNT_{15.3}$-C/C composites; (c) XRD spectra of five composites

pure C/C and $CNT_{3.9}$-C/C composites. The pyrocarbon in pure C/C composite pronounces the texture along the circumference of carbon fibers, which has relatively small arranging curvature. In contrast, for $CNT_{3.9}$-C/C composites, pyrocarbon shows wavy texture. And even nearly around carbon fiber, the pyrocarbon with littery texture has been found, which looks like isotropic glassy carbon. Only aloof from carbon fiber, the matrix carbon has a similar texture to that of pyrocarbon in C/C composite. And with the CNT content increasing, the zone full of pyrocarbons with littery texture around carbon fiber becomes bigger (as shown in the inset of Fig.3b, the width of the littery texture area is over 5 μm in $CNT_{15.3}$-C/C composite). It indicates that CNTs with extending morphology have strongly affected the deposition behavior of pyrocarbon during CVI.

Powder samples of C/C and CNT-C/C composites were further examined by XRD. Fig.3c shows their XRD patterns. For C/C, $CNT_{1.6}$-C/C, $CNT_{3.9}$-C/C and $CNT_{7.2}$-C/C composites, their Ae values are approximately equal but the (002) peak at about 26° shifts towards big angle orientation with the increase of CNT content. According to Bragg′s law ($d_{002}=\lambda/\sin(2\theta)$) and Scherrer equation ($L_c=0.9\lambda/(B\cos\theta)$), we can conclude that the average d-spacing value of the carbon (002) plane (d_{002}) has a distinct decrease, meanwhile a big increase for the stack thickness of (002) planes (L_c) with increase of CNTs grown on carbon fibers. This is very interesting that this change is based on the formation of ISO laminar pyrocarbon generally with relatively small crystallite size (including d_{002} and L_c). Actually, according to the Raman results of the pyrocarbons closely near carbon fibers in five composites (the Raman spectra of C/C and $CNT_{3.9}$-C/C composites are shown in Fig.3a and 3b, respectively), it can been found that although the I_G/I_D (I_G and I_D indicate the intensities of G and D bonds in Raman spectrum, respectively) values decrease invariably after growing CNTs on carbon fibers, both G and D peaks become more intense and sharper than pure C/C composite, which indicates that, despite a decreased microcrystal order, the average d_{002} value of pyrocarbons deposited near carbon fibers in CNT-C/C composites has a distinct decrease compared with C/C composite[15]. This can be the positive evidence for the decreased d_{002} values of CNT-C/C composites in spite of the deposition of ISO layer pyrocarbon around carbon fibers. Exceptionally, the shift of (002) peak is reversed in $CNT_{15.3}$-C/C composite which might be caused the deposition of pyrocarbons with obvious low optical anisotropy (A_e: 11°) in matrix than other composites (A_e: ~14°).

Although some studies have proposed that ACNTs or spread-out CNTs could act as nuclei of small hydrocarbon molecules and induce small hydrocarbon molecules to align in the direction vertical to the surface of CNTs and form ordered pyrocarbon[4-6], the effect of CNTs inducing the formation of higher-textured pyrocarbon is very limited and even ISO

pyrocarbon has deposited around carbon fiber closely in this work. This might be related to the growing morphology of CNTs. Here, after growing CNTs with radially growing morphology on carbon fibers, a big and disorderly 3D network structure is formed around carbon fibers. It sharply increases the nucleation active sites and infiltration rate of pyrocarbon during CVI because of high specific surface area of CNTs[7], resulting in numerous growing cores and the formation of pyrocarbon particles with small size. Moreover, because of the disorder 3D network, the template for high-textured pyrocarbon deposition becomes more coarse and isotropic, compared with ACNTs and spread-out CNTs. Pyrocarbons have deposited on the surface of CNTs, resulting in the very low-textured ISO laminar one. Obviously, with the increase in CNT content, this effect on pyrocarbon deposition can extend to the area aloof from carbon fibers because of the expansion of 3D CNT-network into distant space. Therefore, in $CNT_{15.3}$-C/C composite, the pyrocarbons deposited among carbon fibers have pronounced very low optical anisotropy. However, after growing CNTs on carbon fibers, π-π conjugated electronic structures (because of the sp^2 hybridization structure of CNTs) are formed in deposition space above carbon fibers, which can efficiently induce similar-structured small polyaromatic molecules to arrange parallel to each other in the direction vertical to the surface of CNTs during CVI[4]. Thus, for CNT-C/C composite, the random stacking of polyaromatic molecules has been decreased dramatically, which further lessens the interplanar spacing between (002) planes and also increases their stack thickness (as shown in Raman results). The effect of CNTs on deposition of pyrocarbon during CVI could be shown schematically in Fig.4.

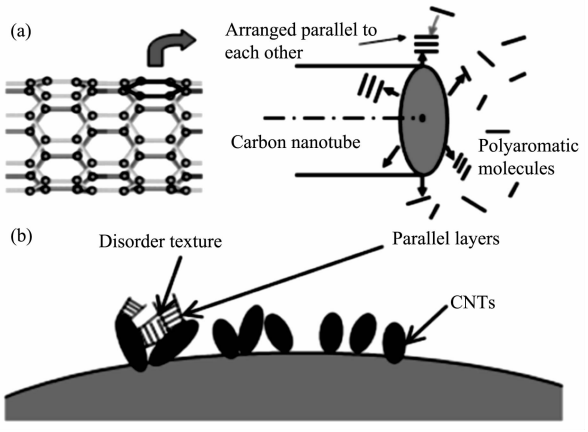

Fig.4　Effect of CNTs on the deposition of pyrocarbon during CVI: (a) π-π structures attract polyaromatic molecules to arrange parallel to each other in the direction vertical to the surface of CNTs, causing decreased d_{002}, (b) CNTs with random orientation induce the formation of pyrocarbon with disorderly texture (i.e. ISO pyrocarbon)

2.3　Influence of CNTs on mechanical strength and fracture behavior of C/C composite

Fig.5a shows typical compressive stress-strain curves of five composites with an apparent density of about 1.65 g·cm^{-3}. After growing CNTs on carbon fibers, the compressive strength/modulus of $CNT_{1.6}$-C/C, $CNT_{3.9}$-C/C, $CNT_{7.2}$-C/C and $CNT_{15.3}$-C/C composites,

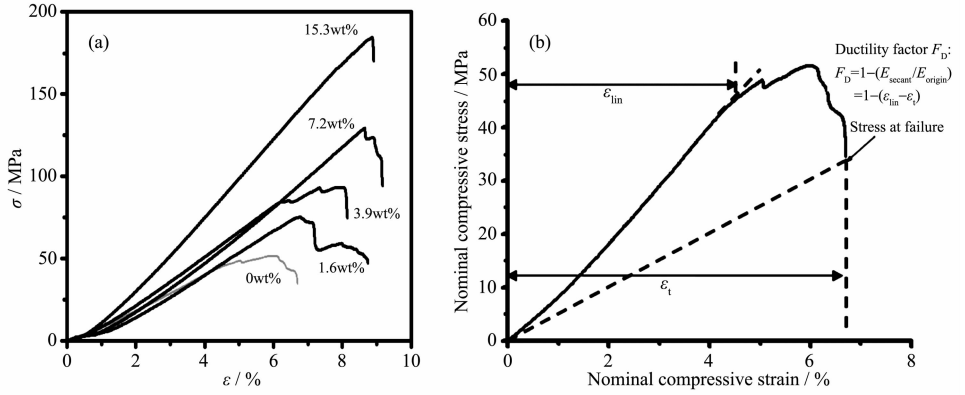

Fig.5　(a) Stress-strain curves of C/C composites with different CNT contents; (b) Definition of F_D:F_D is calculated from the ratio of the secant modulus (the slope of the line from the origin to the stress at failure in the stress-strain curve) to the elastic modulus (the slope of the linear part of the stress-strain curve)

compared to pure C/C composite, increases by 39.3/15.9%, 77.2/37.2%, 137.8/66.4% and 230.6/94.7%, respectively, as shown in Table 1. It indicates the very outstanding reinforcement role of *in-situ* grown CNTs. However, from the curves, we can also see that the fracture mode changes from pseudo-plastic fracture to brittle facture with the increase of CNTs grown on carbon fibers.

Although the mechanical strength of C/C composites is one of the most important keys, the fracture behavior is also a necessary point for the practical applications of C/C composites. In this work, a ductility factor F_D (as shown in Fig.5b) was adopted to evaluate the quasi-ductile fracture behavior of different samples[3]. The results are shown in Table 1. The value of F_D decreases after introducing CNTs and becomes small rapidly with the increase of CNT content. Especially when 15.3wt% CNTs hybridizes carbon felt, the corresponding C/C composite has an over 96% decrease in the value of F_D, compared with pure C/C composite. And the fracture demonstrates very catastrophic. It indicates that CNTs grown on the surface of carbon fibers can not increase the toughness of pyrocarbon-based C/C composite as described in ceramic matrix composites (CMC)[16] but bring about very brittle fracture when the CNT content is relatively high.

For all five composites, the fracture penetrates the height of samples forming about 45-degree angle with the force-accepted plane. And with CNTs increasing, the amount of crushed carbon fragments has an obvious decrease, indicating the reinforced pyrocarbon matrix by CNTs. Fig.6a shows the SEM morphology of the fracture surface of pure C/C composite. A rough fracture surface can be seen and the fibers are pulled out with long length. The cracks between fiber and matrix are distinct, indicating a much weaker interface bond. In contrast, for CNT-C/C composite (especially when the CNT content is relatively high), they exhibit a brittle fracture with a flat fracture surface and very short pulling-out of fibers (Fig.6b shows the fracture surface of $CNT_{7.2}$-C/C composite) and the fiber/matrix interface is more compact and shows no cracks, implying a strong interface bond. Meanwhile, from magnified SEM image of fiber/matrix interface (Fig.6b inset), many tightly-wrapped CNT sprouts by pyrocarbons with very short length (<1 μm) have been found in matrix, which implies strong interfacial bonding between CNTs and the matrix pyrocarbon and also indicates CNTs as bridges between cracked pyrocarbons just like the role of carbon fibers during fracture. In addition, according to SEM results, abundant spherical or cone-shaped pyrocarbons are evident and the size and thickness of them are much

Table 1 Mechanical properties of five composites

Composites	C/C	1.6% CNT-C/C	3.9% CNT-C/C	7.2% CNT-C/C	15.3% CNT-C/C
Compressive strength / MPa	54.5±3.1	75.9±2.6	96.6±4.5	129.6±3.8	180.2±10.0
Modulus / GPa	1.13±0.5	1.31±0.1	1.55±0.3	1.88±0.2	2.2±0.3
F_D	0.243±0.030	0.226±0.016	0.218±0.011	0.056±0.005	<0.010

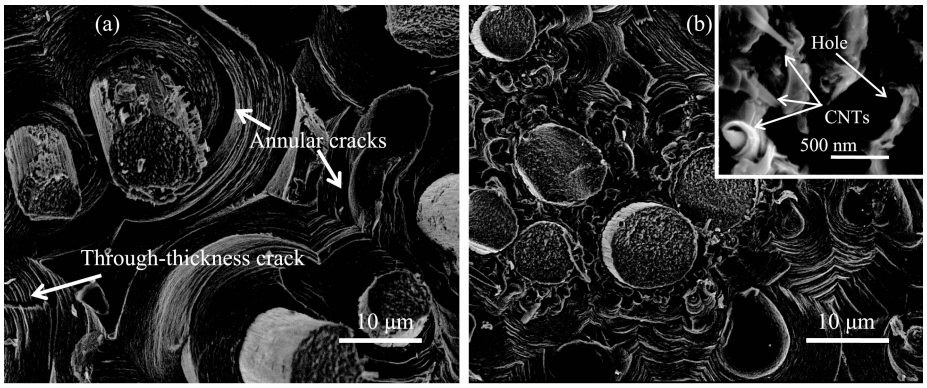

Fig.6 SEM micrographs of fracture surfaces of different composites: (a) A rough and step-like surface in C/C composite; (b) A flat surface in $CNT_{7.2}$-C/C composite (inset is the drawn CNT-sprouts in fracture surface)

smaller and there is nearly no cracks (annular cracks or through-thickness cracks) in them after introducing CNTs, further indicating the reinforcing effect of CNTs on pyrocarbon matrix. On one hand, the growth of CNTs on carbon fibers makes quantities of nucleation active sites for pyrocarbon sharp increase during CVI. This not only accelerates the infiltration rate but also induces the abundant formation of spherical or cone-shaped pyrocarbons, which efficiently inhibits the excessive growing-up of some single pyrocarbons in size and thickness and decreases the probability of cracks occurred in matrix due to thermal stress during fabrication and graphitization and thus enhances the anti-destroying capacity. On the other hand, CNTs grown on carbon fibers also improve the fiber/matrix interface bond efficiently (it profits from the great pull force during preparation provided by CNTs) and reinforce matrix pyrocarbon by bearing loading directly, which increases the resistance for crack propagating in fiber/matrix interface area and matrix. Both of them are beneficial to the increase of mechanical strength. As for the great change in fracture behavior, it can be attributed to the increased fiber/matrix interface bonding and the chaining effect of the big 3D CNT network on pyrocarbon matrices[8], further resulting in relatively brittle failure of C/C composite[17]. Therefore, when CNT content increases and the 3D network of CNTs becomes dense and big, the chaining effect on pyrocarbon matrix also becomes very much forceful, resulting in extreme brittleness and the catastrophic fracture, as shown in $CNT_{15.3}$-C/C composite.

3 Conclusions

CNTs with a uniform growing and extending morphology are in situ grown on carbon fibers in felt. After growing CNTs on carbon fibers, a bulky and disorder 3D network structure is formed above carbon fiber. Under the effect of this network, a thick ISO pyrocarbon layer has deposited closely around carbon fiber and the microcrystal order of pyrocarbon here becomes much lower. According to XRD results, however, the d_{002} values of CNT-C/C composites become much smaller than C/C composite.

In situ grown CNTs have a remarkable influence on mechanical performance of C/C composite. A very small content (1.6wt%) of CNTs in pure felt can elevate the mechanical strength efficiently (by 39.3%). And with increasing CNTs, the mechanical strength and modulus of C/C composite increase quickly. However, the ductility of C/C composite deteriorates sharply and the fracture mode changes from pseudo-plastic fracture to brittle fracture.

Acknowledgements: This work was supported by the National Natural Science Foundation of China under Grant No. 50832004, National 973 Project (Grant No.2011CB605806) and the Research Fund of State Key Laboratory of Solidification Processing (NWPU), China (Grant No.25-TZ-2009).

References:

[1] Fitzer E, Manocha L M. *Carbon Reinforcements and Carbon/carbon Composites*. Berlin: Springer, **1998**:250

[2] Savage G. *Carbon-carbon Composites*. London: Chapman & Hall, **1993**:331

[3] Guellali M, Oberacker R, Hoffmann M J. *Carbon*, **2005**,**43**(9): 1954-1960

[4] Gong Q M, Li Z, Bai X D, et al. *Compos. Sci. Technol.*, **2005**, **65**(7/8):1112-1119

[5] Gong Q M, Li Z, Zhang Z Y, et al. *Tribology International*, **2006**,**36**(9):937-944

[6] Chen J, Xiong X, Xiao P. *Mater. Chem. Phys.*, **2009**,**116**(1): 57-61

[7] Li J S, Luo R Y. *Mater. Sci. Eng. A*, **2008**,**480**(1/2):253-258

[8] Li J S, Luo R Y. *Composites A*, **2008**,**39**(11):1700-1704

[9] Esawi A M K, Farag M M. *Mater. Design*, **2007**,**28**:2394-2401

[10]Qian H, Bismarckb A, Greenhalghc E S, et al. *Composites A*, **2010**,**41**(9):1107-1114

[11]PENG Feng(彭峰), JIANG Jian-Cheng(江剑城), LEI Jian-Guang(雷建光). *Chinese J. Inorg. Chem.* (*Wuji Huaxue Xuebao*), **2002**,**18**(2):190-192

[12]TANG Chang-Xing(唐长兴), QU Mei-Zhen(瞿美臻), ZHOU Gu-Ming(周固民), et al. *Chinese J. Inorg. Chem.* (*Wuji Huaxue Xuebao*), **2003**,**19**(9):1025-1029

[13]KUANG Yun-Hua(况云华), LI Ke-Zhi(李克智), LI He-Jun(李贺军), et al. *Chinese J. Inorg. Chem.* (*Wuji Huaxue Xuebao*), **2009**,**25**(6):951-955

[14]Reznik B, Huttinger K J. *Carbon*, **2002**,**40**(4):621-624

[15]Nakamizo M, Kammereck R, Walker P L. *Carbon*, **1974**,**12** (3):259-267

[16]William A C, Brian W S. *Mater. Today*, **2004**,**7**(11):44-49

[17]Ahearn C, Rand B. *Carbon*, **1996**,**34**(2):239-249